ACS Macro Letters

Letter

pubs.acs.org/macroletters

Solid-State Polycondensation via Ionic-to-Covalent Bond Transformation to Control Polymer Structure: Preparation of Porphyrin-Based Ladder Polymer

Masato Suzuki,*,† Kohei Yokota,† Hiroe Tsuchida,† Kazuhisa Yamoto,† Masayuki Nagata,† Shin-ichi Matsuoka,† Koji Takagi,† Kohei Johmoto,‡ and Hidehiro Uekusa‡

†Department of Materials Science and Engineering, Nagoya Institute of Technology, Gokiso-cho, Showa-ku, Nagoya 466-8555, Japan

‡Department of Chemistry and Materials Science, Tokyo Institute of Technology, O-okayama 2-12-1, Meguro-ku, Tokyo 152-8551, Japan

Supporting Information

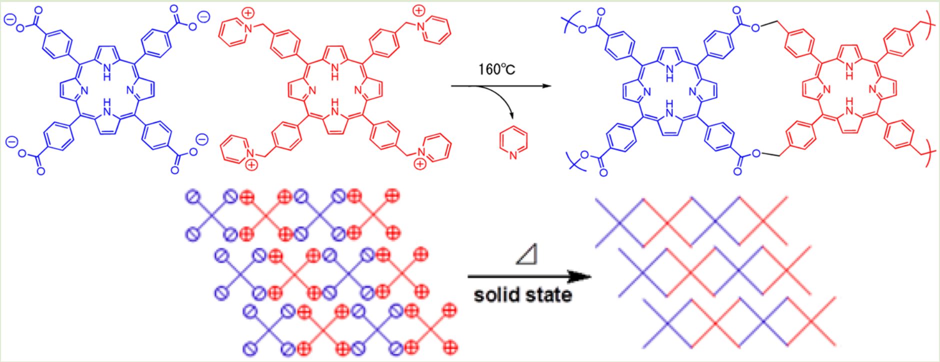

ABSTRACT: The controlled formation and the regular arrangement of polymer chains have been performed by novel solid-state polycondensation including the ionic-to-covalent bond transformation in the ionic molecular crystals. The combination of the tetra-anion and -cation of tetraphenylporphyrin derivatives, tetrakis(benzylpyridinium carboxylate), was found to form layered crystal structures and underwent thermal solid-state polycondensation, thus, releasing the pyridine and forming the benzyl ester linkages. Powder X-ray diffraction, when compared to the monomer crystal structure data, suggested that the ladder polymer was produced with a layered structure.

The crystal-to-crystal transformation of monomer to polymer, termed topochemical polymerization,[1] is an effective tool to achieve not only the controlled formation, but also the regular arrangement of polymer chains. Regular arrangement of monomer molecules in the crystal is fixed by the polymerization. For instance, there are successfully prepared unique polymers with layered structures having intercalation properties[2,3] or with 2D cross-linking.[4,5] Including these examples, most of the topochemical polymerizations are photochemical reactions of limited monomers, tightly restricted by the crystal structures of the monomers.[1,2] We have been exploring the widely applicable solid-state polymerization to control the polymer structures. Our strategy is to utilize the electrostatic interaction for arranging multianionic and -cationic monomer molecules in crystals and then to polymerize them through an ionic-to-covalent bond transformation[6] in the solid-state. In this context, the key reaction designed herein is the thermal solid-state transformation of benzylpyridinium carboxylate to benzyl ester along with generating the pyridine. Accordingly, the present system is a solid-state polycondensation, which seems to be rather inconvenient to use the molecular arrangement in monomer crystals for the regular arrangement of the product polymer chains, since small molecules are liberated along with the polymerization. However, a literature survey revealed that polythiophenes possessing some ordered arrangement is produced by the solid-state debromination polycondensation of the dibromothiophene derivatives.[7,8] In our project, we expect that the electrostatic interaction among monomer molecules in the crystals can work to locate reaction sites close to each other and minimize the molecular movement for the polymerization, effectively memorizing the molecular arrangement in the monomer crystals. In this communication, the tetra-anion and -cation combination of square planar molecules, that is, tetraphenylphorphyrin derivatives, is employed as the monomer (Scheme 1), since their symmetrical shapes are suitable for the initial study. In addition, the polymer incorporating porphyrin rings has a potential to show photo- and electro-

Received: January 6, 2015
Accepted: January 29, 2015
Published: January 30, 2015

DOI: 10.1021/acsmacrolett.5b00013
ACS Macro Lett. 2015, 4, 247−250

Scheme 1. Solid-State Polycondensation, Including Ionic–Covalent Transformation

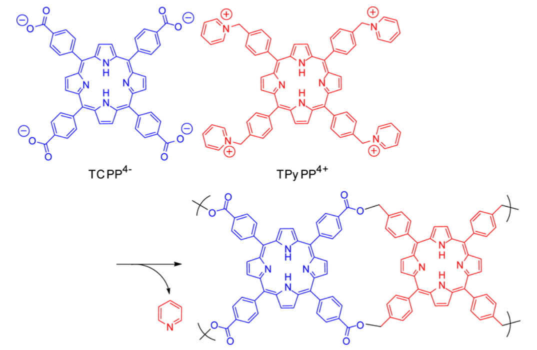

chemical functionality, which is dependent on their intra- and intermolecular arrangement.

The known compounds, meso-tetrakis(4-carboxy-phenyl)- and meso-tetrakis[(4-bromomethyl)phenyl]-porphyrins,[9,10] were converted to the tetra-anionic and -cationic compounds ($TCPP^{4-}(Bu_4N^+)_4$ and $TPyPP^{4+}Br^-{}_4$) by the treatment with tetrabutylammonium hydroxide and pyridine, respectively. The objective combination salt ($TPyPP^{4+}TCPP^{4-}$) was obtained by the ion-exchange between $TCPP^{4-}(Bu_4N^+)_4$ and $TPyPP^{4+}Br^-{}_4$ and purified by recrystallization using vapor diffusion of acetone into the $MeOH/EtOH/H_2O$ solution.

The X-ray diffraction analysis of the single crystal of the prepared $TPyPP^{4+}TCPP^{4-}$ revealed an interesting molecular arrangement (Figure 1).[11] Two kinds of porphyrins, $TPyPP^{4+}$ and $TCPP^{4-}$, alternately align along the *a*-axis, and the same species of porphyrin are in line along the *c*-axis. They form the layers, each of which stacks along the *b*-axis with shifting by half a porphyrin molecule along the *a*-axis. Each layer has three kinds of cavities, one of which is occupied with the pyridinium groups from the adjacent layers (Figure 1b) and others of which are filled with solvents such MeOH, EtOH, and H_2O. The reaction sites, the benzylic carbon atom and the carboxylate oxygen atom, are located close to each other (distance = 318 and 320 pm).

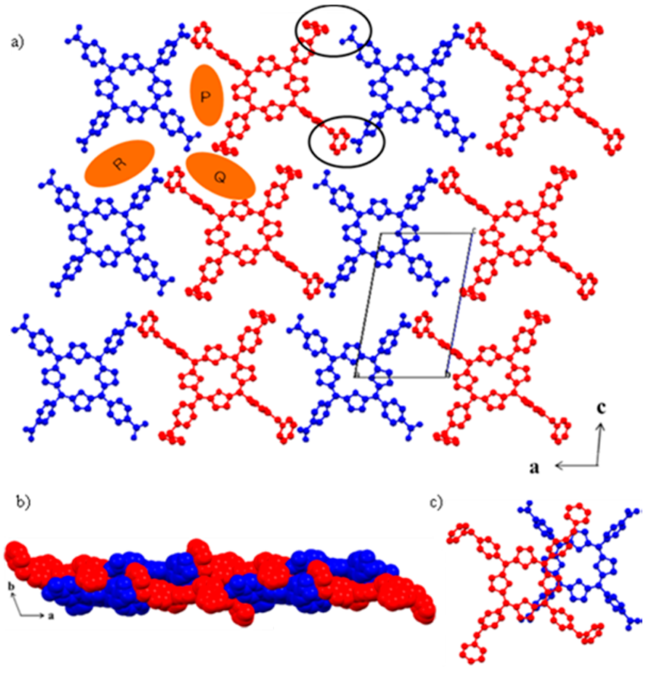

Figure 1. Crystal structures of $TPyPP^{4+}TCPP^{4-}$ recystallized by vapor diffusion of acetone into the $MeOH/EtOH/H_2O$ solution: (a) one layer on the a–c plane, (b) the packing between the layers along the *b* axis, and (c) the stacking of $TPyPP^{4+}$ and $TCPP^{4-}$ between the layers. There are three kinds (P, Q, and R) of cavities in the layer; cavities P and Q are filled with solvents such as MeOH, EtOH, and H_2O, which are omitted, and cavities R are occupied with the pyridinium groups from the adjacent layers as shown in (b). Representative reaction sites are highlighted by the ovals.

The thermal reactivity of $TPyPP^{4+}TCPP^{4-}$ was investigated by thermogravimetry and differential thermal analyses (TG-DTA) of the powdered crystals (Supporting Information, Figure S1). There are two observed stages for the endothermic weight loss; the first one observed at less than 100 °C is due to vaporization of the solvents included in the crystals, and the second that starts around 160 °C is reasonably ascribable to the objective reaction. The weight loss observed at the second stage is in good agreement with the theoretical value (18%) due to the elimination of the pyridine. Thus, the crystal powder of $TPyPP^{4+}TCPP^{4-}$ was heated at 160 °C under N_2 and subjected to IR spectroscopy (Figure S2). Observed are the characteristic absorption peak due to the ester carbonyl group appearing at 1715 cm^{-1} and that due to the carboxylate anion disappearing at 1570 cm^{-1} after 14 h, suggesting the formation of the ester from the benzylpyridinium carboxylate.[12] The product polymer was hardly soluble in any solvent such as DMF, DMSO, $(CF_3)_2CHOH$, and CF_3CO_2H.

An optical microscopic analysis was performed for the $TPyPP^{4+}TCPP^{4-}$ crystals, which were prepared by casting the MeOD-EtOH-H_2O solution on a glass plate and drying under acetone vapor (Figure S3). The formed red needle-like crystals were heated on the glass plate at 160 °C under N_2 for 14 h. The microscopy with a pair of cross polarizers showed the anisotropy even for the reaction product (Figure S3). IR spectroscopy of this sample also proved the transformation of the carboxylate anion into the ester linkage.

A powder X-ray diffraction (XRD) measurement was employed to obtain more information about the polymerization product. The supernatant liquid from the vapor diffusion recrystallization of $TPyPP^{4+}TCPP^{4-}$ was replaced with acetone, in which the crystals were vigorously stirred. The fractured crystals were spread onto a glass plate used for the XRD measurement and then air-dried. This sample was subjected to the XRD measurement before and after heating at 160 °C for 14 h on an aluminum plate heater under N_2 (Figures. 2b and 2e). Even after heating, the sharp diffraction peaks are observed in the low angle area of less than 10°, while the peaks in the higher angle area are broad (Figure 2e). This finding is consistent with the optical microscopy showing anisotropy, as already mentioned (Figure S3), and reasonably suggests that the product polymer would maintain the coarse regularity from relative positions of the monomer molecules in the crystals, however, losing the fine regularity from the conformation.

For further discussions, the powder XRD pattern of the $TPyPP^{4+}TCPP^{4-}$ crystals (Figure 2b) was compared to that mathematically obtained from the single crystal structure data, as shown in Figure 1 (Figure 2a). There is a significant difference between these two patterns, suggesting that the crystal structure of the air-dried sample is not identical to that in Figure 1. Accordingly, the powder XRD measurement was performed for the wet sample using a rotating glass capillary containing the $TPyPP^{4+}TCPP^{4-}$ crystals fractured in acetone.

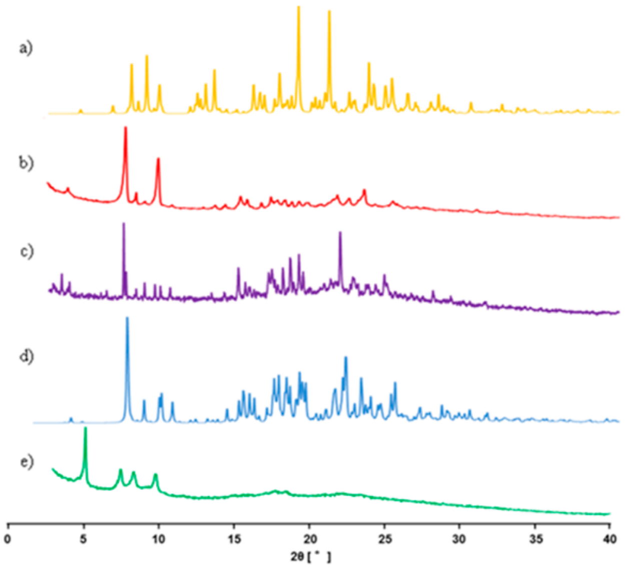

Figure 2. XRD patterns (a) given by mathematical transformation of the single crystal structure data of Figure 1, (b) measured using air-dried TPyPP^{4+}TCPP^{4-} crystals on a glass plate, (c) measured using TPyPP^{4+}TCPP^{4-} crystals in acetone in a glass capillary, (d) given by mathematical transformation of the single crystal structure data of Figure 3, and (e) measured for the polymer that were produced by heating TPyPP^{4+}TCPP^{4-} crystals on a glass plate at 160 °C for 14 h.

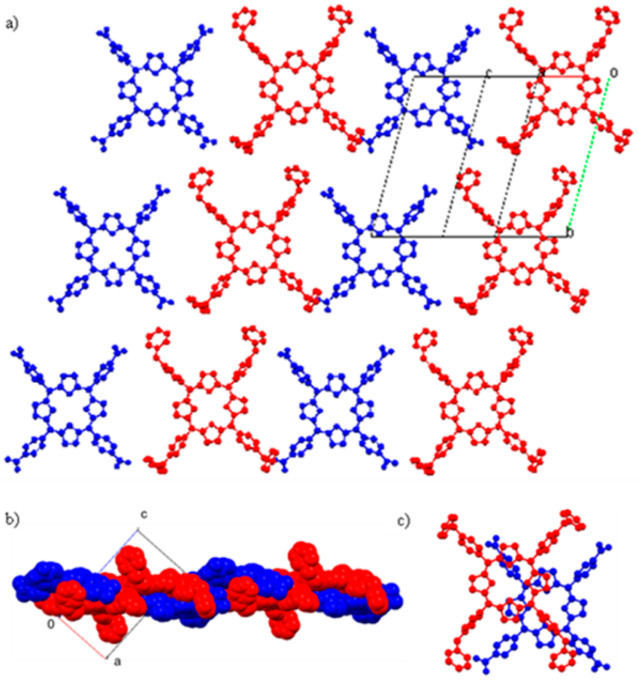

Figure 3. Crystal structures of TPyPP^{4+}TCPP^{4-} recystallized by vapor diffusion of acetone into the MeOH/EtOH/H_2O solution and then soaked in acetone: (a) one layer along the *b* axis, (b) the packing between the layers on the a−c plane, and (c) the stacking of TPyPP^{4+} and TCPP^{4-} between the layers. Solvents in cavities are omitted.

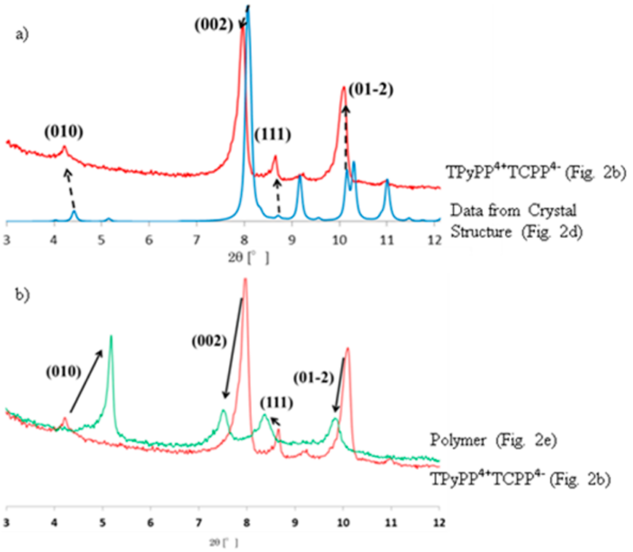

Figure 4. (a) Assignment of Miller indices for XRD peaks of TPyPP^{4+}TCPP^{4-} on the basis of the crystal structure data shown in Figure 3 and (b) shift of the assigned peaks by the polymerization.

However, the resultant data (Figure 2c) were also inconsistent with the peak pattern from the crystal structure in Figure 1 (Figure 2a). Fortunately, a small single crystal in acetone was found to be applicable for the crystal structure measurement, consequently, showing another crystal structure of TPyPP^{4+}TCPP^{4-} (Figure 3).[13] It was concluded that soaking the crystals in acetone gives rise to a slight change in the original crystal structure by replacing the solvents in the crystal cavities with acetone and H_2O. Two crystal structures in Figures 1 and 3 show a difference in the stacking of the layers and the conformation of the functional groups. The distances between the reaction sites become longer in Figure 3, being 320, 326, 426, and 490 pm. This crystal structure was also mathematically transformed into the powder XRD pattern (Figure 2d), which is reasonably consistent with that measured in the capillary (Figure 2c). The difference in relative peak intensity between them is ascribable to the measurement using the small crystals without grinding. The peaks in Figure 2c are observed at slightly lower angle positions when compared to the corresponding ones in Figure 2d due to the difference in the measurement temperatures, r.t. and −180 °C for Figure 2c and d, respectively. Since there is a reasonably observed similarity between the XRD patterns of the air-dried and wet samples (Figure 2b,c), one can discuss the solid-state polymerization based on the monomer crystal structure shown in Figure 3.[14] Accurate Miller indices are mathematically assigned to each of the peaks in Figure 2d from the single crystal data, so that the peaks in the low angle area in Figure 2b can be assigned with the Miller indices by the comparison with Figure 2d. This peak assignment shown in Figure 4a was performed by considering the peak shift observed between Figure 2c and Figure 2d, as mentioned above. These assigned peaks for the monomer crystal allow discussing the XRD peaks of the product polymer in Figure 2e. It is reasonably elucidated that these peaks would undergo some shift through the solid-state polymerization (Figure 4b). As seen in Figure 3, the polymerization would reasonably take place along the alternate alignment of TPyPP^{4+} and TCPP^{4-} in the crystal. The spacing between the (010) planes that are parallel to this alignment reasonably shrinks through the polymerization, consequently causing the corresponding XRD peak shifting to the higher angle position, since the pyridines that are located in the cavities between the (010) planes are released (Figure 5a). As shown in Figure 5b, the reaction sites overlap with each other in the layer, so that the spacing between the (002) planes

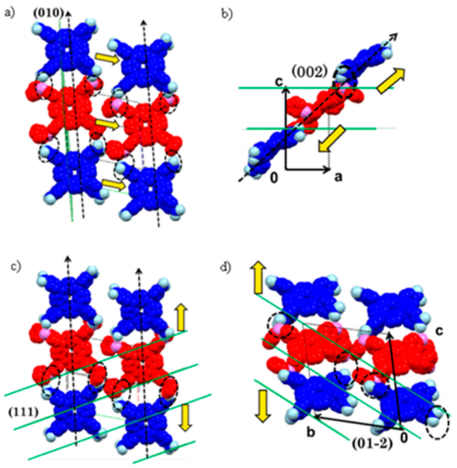

Figure 5. Movement of monomer molecules by the polymerization; views cut perpendicularly to (a) (010), (b) (002), (c) (111), and (d) (01−2) planes.

expands through the polymerization. Similarly, two other plane spacings shown in Figure 5c,d are enlarged. The XRD peaks due to these three planes shifting to the lower angle positions are observed (Figure 4b). Accordingly, it is concluded that the solid-state polymerization of $TPyPP^{4+}TCPP^{4-}$ takes place by roughly maintaining the positional relationship of the monomer molecules in the crystals. The product polymer has a ladder structure (Scheme 1) and forms a layered stacking with each other in the solid state.[15]

While the square planar monomers were employed in this study, our studies are ongoing by using the same strategy for other molecules with different topologies. We believe that the electrostatic interaction in monomer crystals would be widely and effectively applicable to solid-state polymerization, giving rise to a regular arrangement of not only linear, but also cross-linked polymers.

■ ASSOCIATED CONTENT

Ⓢ Supporting Information

Experimental details and supplementary data. This material is available free of charge via the Internet at http://pubs.acs.org.

■ AUTHOR INFORMATION

Corresponding Author

*E-mail: suzuki.masahito@nitech.ac.jp.

Notes

The authors declare no competing financial interest.

■ ACKNOWLEDGMENTS

This work was supported by JSPS KAKENHI Grant Number 21550117.

■ REFERENCES

(1) Dou, L.; Zheng, Y.; Shen, X.; Wu, G.; Fields, K.; Hsu, W.-C.; Zhou, H.; Yang, Y.; Wudl, F. *Science* **2014**, *343*, 272 and references therein..

(2) Matsumoto, A.; Odani, T. *Macromol. Rapid Commun.* **2001**, *22*, 1195.

(3) Shimogaki, T.; Matsumoto, A. *Macromolecules* **2011**, *44*, 3323.

(4) Kissel, P.; Erni, R.; Schweizer, W. B.; Rossell, M. D.; King, B. T.; Bauer, T.; Götzinger, S.; Schlüter, A. D.; Sakamoto, J. *Nat. Chem.* **2012**, *4*, 287.

(5) Radha Bhola, R.; Payamyar, P.; Murray, D. J.; Kumar, B.; Teator, A. J.; Schmidt, M. U.; Hammer, S. M.; Saha, A.; Sakamoto, J.; Schlüter, A. D.; King, B. T. *J. Am. Chem. Soc.* **2013**, *135*, 14134.

(6) Ionic-to-covalent bond transformation from the cyclic ammonium carboxylate to ester-amine has been effectively employed for the preparation of unique multi-cyclic polymers in highly diluted solutions. *Topological Polymer Chemistry: Progress of Cyclic Polymers in Syntheses, Properties and Functions*; Tezuka, Y., Ed.; World Scientific: Singapore, 2013.

(7) Meng, H.; Perepichka, D. F.; Bendikov, M.; Wudl, F.; Pan, G. Z.; Yu, W.; Dong, W.; Brown, S. *J. Am. Chem. Soc.* **2003**, *125*, 15151.

(8) Lepeltier, M.; Hiltz, J.; Lockwood, T.; Bélanger-Gariépy, F.; Perepichka, D. F. *J. Mater. Chem.* **2009**, *19*, 5167.

(9) Niedercorn, F.; Ledon, H.; Tkatchenko, I. *New J. Chem.* **1988**, *12*, 897.

(10) Wen, L.; Li, M.; Schlenoff, J. B. *J. Am. Chem. Soc.* **1997**, *119*, 7726.

(11) Crystal data for $TPyPP^{4+}TCPP^{4-}$ recrystallized from the MeOH/EtOH/H_2O solution with acetone: $C_{68}H_{54}N_8 \cdot C_{48}H_{26}N_4O_8 \cdot 2(C_2H_6O_1) \cdot 7.01(C_1H_4O_1) \cdot 2(H_2O_1)$, triclinic, *P*-1, $a = 11.8259(4)$, $b = 14.4335(5)$, $c = 18.5070(5)$ Å, $\alpha = 106.243(1)°$, $\beta = 93.222(1)°$, $\gamma = 111.298(1)°$, $V = 2781.40(15)$ Å^3, $Z = 1$, $\mu = 0.710$ mm^{-1}, final *R* indices $[I > 2\sigma(I)]$: $R_1 = 0.1242$, $wR_2 = 0.3485$, CCDC 1039172.

(12) The solid-state polymerization of dianionic and -cationic monomer combination, 1,5-bis(pyridiniummethyl)naphthalene terephthalate, was also performed. The ionic-to-covalent bond transformation was supported by IR, ^{1}H NMR, and MALDI-TOF-mass spectroscopic analyses of the soluble oligomer. The data will be published elsewhere.

(13) Crystal data for $TPyPP^{4+}TCPP^{4-}$ recrystallized from the MeOH/EtOH/H_2O solution with acetone and then soaked in acetone: $C_{68}H_{54}N_8 \cdot C_{48}H_{26}N_4O_8 \cdot 1.9(C_3H_6O_1) \cdot 11.7(H_2O_1)$, triclinic, *P*-1, $a = 11.7469(2)$, $b = 20.8281(4)$, $c = 22.7225(4)$ Å, $\alpha = 74.7242(7)°$, $\beta = 87.9339(7)°$, $\gamma = 83.4640(7)°$, $V = 5328.02(17)$ Å^3, $Z = 2$, $\mu = 0.738$ mm^{-1}, final *R* indices $[I > 2\sigma(I)]$: $R_1 = 0.0947$, $wR_2 = 0.2572$, CCDC 1039173.

(14) The XRD pattern of the powdered monomer crystals, which were prepared by grinding the single crystals, as shown in Figure 1, was almost identical to that of the air-dried sample in Figure 2b. In addition, the polymers produced from these two samples showed also the same XRD peaks as shown in Figure 2e. These findings suggest that the monomer crystals in Figure 1 are transformed into the crystal structure shown in Figure 3 and then polymerized.

(15) It is hard to deny that there may be involved the defect structures such as the 2D-network and 3D-cross-linking.